

Highlights

The core finding of my paper entitled 'Serviceability of non-prismatic concrete beams: combined-interaction method' are presented below:

- Serviceability behaviour of non-prismatic concrete beams cannot accurately be predicted by the current partial- and full-interaction models presented by previous researchers.
- A new combined-interaction model is proposed in this work which will allow for partial- and full-interaction regions along the beam to be accounted for by calculating the value of slip between reinforcement bars and surrounding concrete.
- The combined-interaction method developed in this work provides good predictions for deflections at serviceability as it takes into account bond-slip effects.
- In general, predictions for the average and maximum crack widths and the number of cracks are reasonably accurate when compared with experimental results.
- Previously, fabric-formed concrete beams have only been studied at the ultimate limit state only. The method put forward in this work will allow that for the first time the relevant serviceability criteria for fabric-formed concrete structures of varying geometry be predicted.

1 **Serviceability of non-prismatic concrete beams:**

2 **combined-interaction method**

3 Yadgar Tayfur, Antony Darby, Tim Ibell, John Orr, Mark Evernden

4 Yadgar Tayfur

5 Doctor of structural engineering, UK (e-mail: Yadgar.tayfur@bath.edu).

6 Antony Darby

7 Reader, University of Bath, Department of Architecture and Civil Engineering, UK (e-mail:

8 a.p.darby@bath.ac.uk).

9 Tim Ibell

10 Professor of Civil Engineering, University of Bath, Department of Architecture and Civil Engineering, UK

11 (e-mail: T.J.Ibell@bath.ac.uk).

12 John Orr

13 Assistant Professor, University of Cambridge, Department of Engineering, UK. (email: jj033@cam.ac.uk)

14 Mark Evernden

15 Senior Lecturer, University of Bath, Department of Architecture and Civil Engineering, UK (e-mail:

16 m.evernden@bath.ac.uk).

17 **Abstract**

18 Interest in the shape optimisation of concrete members is increasing alongside the availability of fabric

19 formwork as a relatively simple technique to cast non-prismatic concrete structures. Research has shown

20 that up 40% of concrete can be saved when shape optimised concrete beams are cast in fabric forms.

21 However, optimisation results in members with non-uniform cross-sections and the resulting beam is less

22 stiff than an equivalent strength prismatic beam. Serviceability, rather than strength, may govern the design

23 of such members and therefore understanding the serviceability behaviour (deflection and cracking) of

24 shape optimised concrete members becomes is a critical design consideration. There are many methods
25 which can be used to evaluate serviceability behaviour of reinforced concrete beams, including the full-
26 interaction method, which assumes no slip between the reinforcement and the surrounding concrete, and
27 the partial-interaction method which accounts for slip. The full-interaction method is based on a smeared
28 crack approach and so is unsuited for the prediction of cracking behaviour. The partial-interaction method,
29 on the other hand, assumes that cracks form through bond-stress transfer only. In the case of non-prismatic
30 concrete beams, the cracking capacity varies along the member. Therefore, cracking can occur over
31 extended regions (full and partial bond interaction regions) and so it can be argued that neither of these
32 models is fully suitable for the prediction of deflections and cracking of shape-optimised concrete beams.
33 In this paper, a novel combined-interaction method is, for the first time, presented to predict the
34 serviceability behaviour of non-prismatic statically determinate concrete beams by simulating both full and
35 partial bond interactions at different cracked and uncracked regions along the length of the member. In
36 order to validate this approach, two non-prismatic simply supported beams were cast and tested. The test
37 results for deflections, crack widths and crack spacings were in good agreement with the predicted results.

38 **Keywords:** Combined-interaction method, Fabric-formed concrete, full-interaction analysis, partial-
39 interaction analysis, serviceability.

40 **1 Introduction:**

41 Fabric formwork, a technique for casting non-prismatic concrete members, has recently brought increased
42 attention to the area of shape optimisation of concrete structures (Veenendal et al., 2011). Figures 1 & 2)
43 show a number of fabric-formed concrete beams and trusses. Shape optimised concrete members use less
44 concrete material than their prismatic counterparts because their shape reflects the requirements of the
45 loading envelope (Bailiss, 2006, Orr, 2012). Such members, generally have smaller cross-sectional
46 dimensions along their length than an equivalent strength prismatic beam (Garbett et al. 2008). However,
47 this makes them significantly less stiff and, in many cases, serviceability criteria rather than strength can
48 govern their design (Tayfur, 2017). Therefore, understanding the serviceability behaviour of non-prismatic
49 fabric-formed concrete members is important.

50



51

52

Figure 1: Fabric-formed concrete (Photos by Mark West: Hawkins et al. 2016)



53

54

Figure 2: Fabric-formed continuous concrete beam cast at the University of Bath (credit Tayfur, 2016)

55

Common methods used to evaluate short-term serviceability behaviour of concrete beams include empirical

56

relationships and sectional analysis. The empirical formula suggested by ACI committee 435 (2000) to find

57

deflections combines cracked and uncracked flexural stiffness to find an effective flexural stiffness (EI_e),

58

and applies this value to the whole beam. These methods are not suitable for optimised non-prismatic beams

59 as flexural stiffness varies significantly along the beam length due to changes in cross-section (and
60 specifically section depth). Therefore, a sectional approach is seen to be more appropriate as it allows every
61 section along the member to be dealt with separately.

62 Sectional analysis methods can be divided into two categories; full-interaction and partial-interaction. The
63 full-interaction method (FI) is based on the assumption of perfect bond in which plane sections remain
64 plane and no slip is assumed between the reinforcement and concrete (Kwak and Kim, 2002). The full-
65 interaction method is unable to predict specific cracking behaviour of concrete beams because the cracks
66 are assumed to be smeared along the cracked region of the member. The partial-interaction method (PI),
67 on the other hand, allows slip to occur between the reinforcement and the concrete (Oehlers et al. 2011,
68 Visintin et al.,2013).

69 Partial-interaction analysis has previously only been applied to prismatic beams (Visintin et al., 2013). The
70 initial crack is formed first under the assumption of full-interaction, and subsequent cracks are assumed to
71 form purely due to partial-interaction (Oehlers et al., 2013). For prismatic simply supported beams under
72 uniformly distributed loading, an initial crack occurs at the point of maximum bending moment, and all
73 other subsequent cracks occur due to concrete-reinforcement bond stress transfer when the tensile strength
74 of the concrete is exceeded. The bending moment value decreases when moving away from the initial crack
75 but the cracking capacity of the beam stays constant, assuming that the sectional properties do not change
76 along the beam length. The primary cracks therefore can only occur through partial-interaction at a point
77 at which the full-interaction region starts.

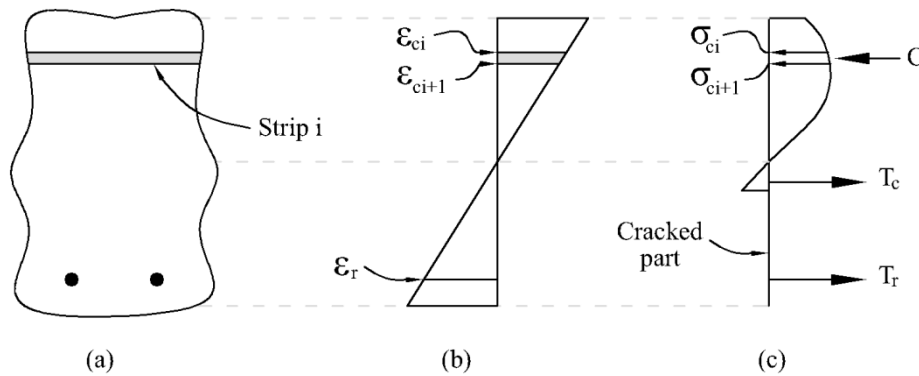
78 Crack development in non-prismatic beams is more complicated since the sectional cracking capacity of
79 the beam is not constant. This, coupled with the variable applied moment, means that cracking can
80 potentially be initiated at any location, and subsequent cracking can occur over extended areas. The
81 formation of these cracks cannot be predicted purely by the partial-interaction method because they form
82 due to a full-interaction mechanism. Conversely, the full-interaction method cannot simulate crack-
83 widening, preventing its use for calculating crack spacing and crack widths. Thus, neither of the interaction
84 models can be applied alone to accurately model the cracking behaviour, and a method that takes into
85 account different interaction regions is required to find the order of crack formation and the location and
86 widths of cracks. Therefore, in this paper, a novel combined-interaction model is developed to

87 simultaneously simulate full and partial interaction behaviour between the reinforcement and the
 88 surrounding concrete by which the behaviour of non-prismatic and statically determinate concrete members
 89 can be predicted.

90 2 Methodology

91 2.1 Full-interaction analysis

92 The full-interaction (FI) model assumes that the member deflects under flexural curvature only, and that
 93 cracks are smeared for the purpose of finding curvatures. Concrete cracks when its tensile strain is
 94 exceeded. Using this model, the moment-curvature relationship at every section of the member is found
 95 step by step, by dividing each section into a number of horizontal strips, Figure 3. Increments of curvature
 96 can be applied gradually while adjusting the neutral axis to ensure equilibrium in order to determine the
 97 moment of resistance.



98

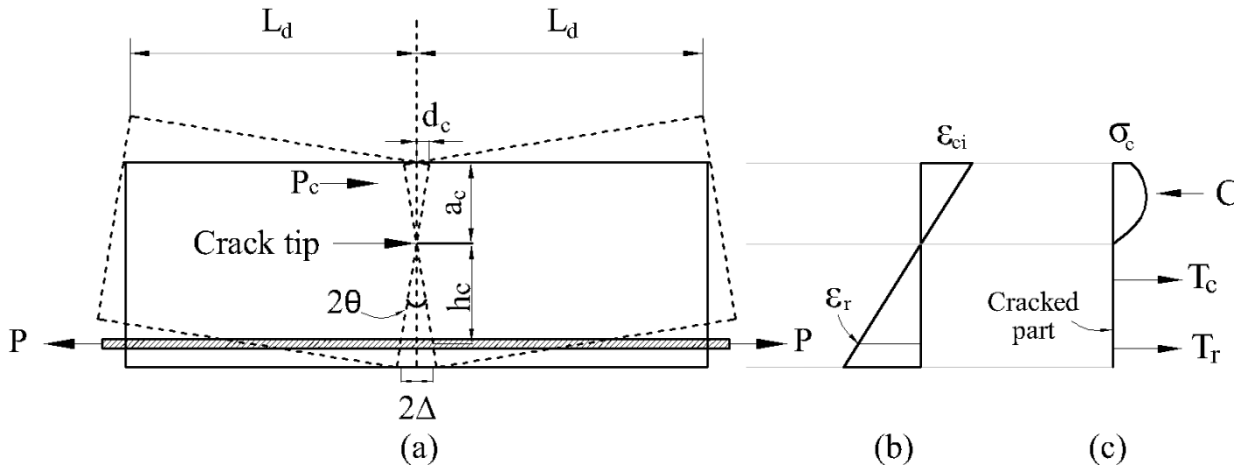
99 Figure 3: Full-interaction analysis (a) discretised section, (b) strain profile, (c) stress profile

100 2.2 Partial-interaction analysis

101 The partial-interaction model was previously developed by Visintin et al. (2013) to evaluate the moment-
 102 rotation relationship at any section using a numerical procedure that finds the relationship between the
 103 force in the reinforcement, P , and the slip Δ . This sectional-segmental analysis model assumes an initial
 104 crack already exists in the beam, the location of which can be found initially from full-interaction analysis.
 105 Following the initial crack, the partial-interaction method is able to track the formation and propagation of
 106 primary, secondary and tertiary cracks under increasing load (for prismatic beams). A primary crack is a

107 crack which forms due to reinforcement-concrete bond-stress transfer where the full-interaction boundary
 108 conditions are met, which is where the slip and slip-strain values are zero at the same point. A secondary
 109 crack occurs between two existing cracks where the slip value is zero but slip-strain has a non-zero value.
 110 At latter stages of loading, and if the reinforcement–concrete bond strength suffices, tertiary cracks may
 111 form between two secondary cracks.

112 The $P - \Delta$ relationship is found from partial-interaction analysis at a cracked section, and a sectional
 113 analysis procedure is then employed to find the moment-rotation relationship. As shown in Figure 4, the
 114 formation of a crack introduces a rigid-body rotation, 2θ , in the cracked region due to crack opening 2Δ
 115 (equal to the slip of the reinforcement), and an associated displacement in the compression part of the
 116 concrete equal to $2d_c$. The variation of deformation in the compression part of the concrete is assumed to
 117 be linear, and d_c is proportional to the value of slip at the crack and neutral axis depth (Oehlers et al., 2013).



118
 119 Figure 4: (a) Deformations at a crack, (b) Strain profile, (c) Stress distribution

120 Initially, the depth to the neutral axis a_c is estimated, so that the deformation in the concrete d_c and the
 121 moment corresponding to the rotation θ can be calculated from the transformed section as follows:

$$122 \quad d_c = \frac{\Delta}{(d - a_c)} a_c \quad (1)$$

123 The deformation in the concrete d_c can be converted to a strain profile by dividing it by the deformation
 124 length L_d , which is taken as equal to half of the crack spacing (distance between two subsequent cracks):

125
$$\varepsilon_c = \frac{d_c}{L_d} \quad (2)$$

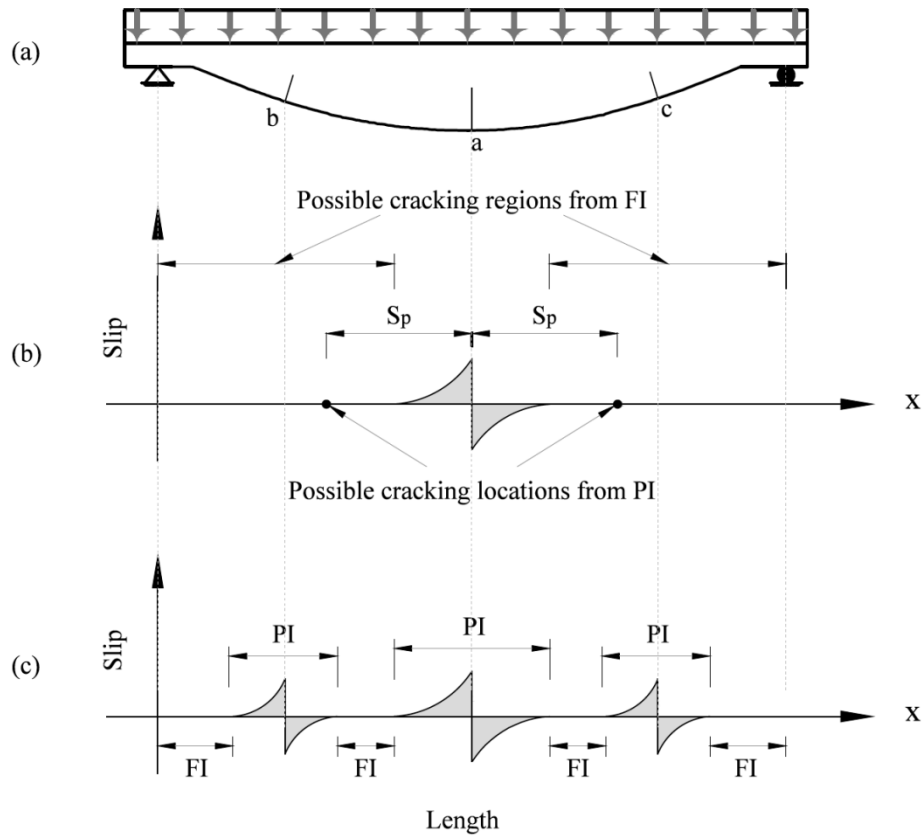
126 Once the strain profile is obtained, the same sectional analysis procedure defined previously for full-
127 interaction analysis can be applied iteratively to find the correct value of the initially estimated a_c , and
128 subsequently to determine the value of moment M induced by the slip Δ .

129 **2.3 Combined-interaction method**

130 **2.3.1 Cracking**

131 A new combined interaction method is developed in this paper to predict cracking and deflections for non-
132 prismatic concrete beams. In the pre-cracking stage, full-interaction analysis is applicable to find
133 deflections and predict the location of the initial cracks and the bending moment at which each crack forms.
134 At later stages of cracking, a partial bond interaction at the vicinity of cracks (where slip is not zero) and
135 full bond interaction elsewhere along the beam is seen. Therefore, subsequent cracks may either be
136 identified through full- or partial-interaction methods.

137 Figure 5 illustrates the cracking process of a non-prismatic beam within the different interaction regions.
138 Assuming that a is an initial crack discovered through full-interaction analysis, in Figure 5(a), then the slip
139 distribution between the reinforcement and the concrete to the left and right of the crack is as shown in
140 Figure 5(b). The next crack occurs when either 1) the applied bending moment at the initial crack results
141 in a stress transferred to the concrete via bond-slip and partial-interaction mechanism to cause a crack at
142 the primary crack spacing distance (S_p); or 2) the applied bending moment exceeds the cracking moment
143 capacity (M_{Crf}) anywhere in the full-interaction region where slip is zero. In this stage, b and c are the two
144 possible cracks on either side of the initial crack a that may form based on one of mechanisms given above.



145

146 Figure 5: Cracking process in the proposed combined-interaction method: (a) Optimised concrete beam,
 147 (b) Initial crack, (c) Three cracks

148 Similarly, as shown in Figure 5(c), the next crack may occur somewhere in the remaining full-interaction
 149 regions, marked as FI, where the ratio of applied moment (M_A) to cracking moment capacity (M_{crf}), (
 150 M_A/M_{crf}), is largest, or in the partial-interaction regions, marked as PI, where the applied moment at one
 151 of the cracked sections exceeds the moment required to cause a crack through bond-stress transfer, (M_{Crp}).

152 The moment-curvature behaviour of the cracked sections depends mostly on their distance from
 153 neighbouring cracks (i.e. bond stress transfer length). Larger crack spacing results in higher total bond
 154 stress transfer and eventually larger slip values at the same load level when compared with closer crack
 155 spacing, provided that the crack spacing is smaller than S_p . Furthermore, the value of bending moment at
 156 which a section cracks due to partial-interaction depends on the distance over which the bond stress transfer
 157 occurs. Likewise, the locations of cracks formed in the full- or partial-interaction regions at various stages
 158 of loading dictate where the next generation of cracks will appear, and eventually how the beam will behave
 159 in the later stages of loading. A numerical procedure for the work presented was adopted in this paper in

160 which a ‘register-eliminate’ algorithm was developed to predict the cracking process of non-prismatic
161 concrete beams based on the proposed combined-interaction method.

162 *Register-eliminate algorithm*

163 In this procedure, a generation of possible cracks were found in each step of loading based on both
164 interaction approaches (smeared cracks from full-interaction analysis and discrete cracks from partial-
165 interaction analysis). The algorithm was designed to iteratively eliminate less possible cracks (according
166 to the PI and FI analysis described below) in the calculations and register actual cracks among these
167 possible cracks based on the highest possibility. The term “actual crack” is used here for the resulting
168 cracks which are predicted to occur.

169 The procedure was automated in MATLAB. In the first step, the concrete beam is divided into a number
170 of sections. The moment-curvature and load-slip relationship for each section are found based on full- and
171 partial-interaction analysis respectively. In the partial-interaction analysis described earlier, subsequent
172 cracks are assumed to form at a certain distance from an existing crack. These distances are limited to the
173 primary, secondary or tertiary crack spacing. However, in the combined-interaction method, since crack
174 locations are predicted by both interaction models rather than just partial-interaction, crack spacing can
175 vary. Therefore, the $P - \Delta$ relationship is developed for each section based on a range of possible crack
176 spacing, from closest to farthest possible crack spacing. The closest possible crack spacing is found based
177 on the smallest slip distribution length possible once a crack forms. This is because theoretically no crack
178 will form within the close neighbourhood of an existing crack where slip is not zero. The farthest possible
179 crack spacing is taken as the maximum bond-slip development length because if a crack is further than this
180 distance from an existing crack, it will have no effect on the $P - \Delta$ relationship of the existing crack.

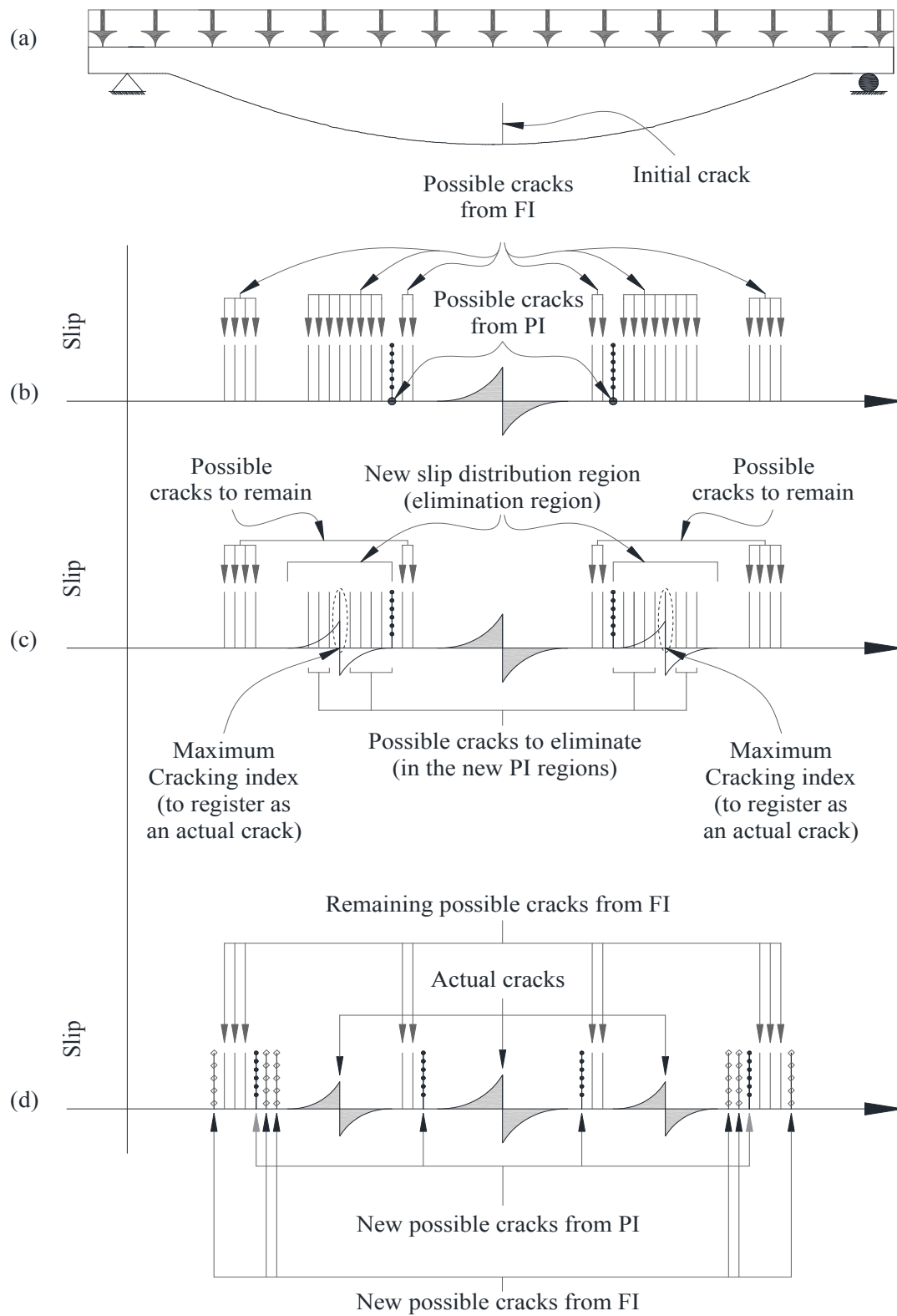
181 In the next step, increments of load are applied to the member gradually and the deflection profile is
182 calculated based on full-interaction bond assumption up until the onset of the initial crack. The vicinity
183 length (the length of slip distribution region on the left and right-hand sides of the crack) of the initial crack
184 is then found. Outside this region, locations of possible cracks are found using full-interaction analysis.
185 This is done by introducing a cracking index which is equal to the ratio of the applied moment M_A to the
186 cracking moment capacity M_{crf} at each section. Any section with a full-interaction cracking index

187 M_A/M_{crf} larger than unity indicates a possible crack. Possible cracks based on the partial-interaction
188 method are also found (if any) by finding the applied moment M_A at the cracked section and also the
189 moment needed at the crack to cause another crack to form through a partial-interaction mechanism M_{crp} .
190 If the partial-interaction cracking index M_A/M_{crp} is larger than unity then a possible crack location is
191 indicated. Figure 6a through 6d shows the procedure of eliminating possible cracks and registering actual
192 cracks at two consecutive post-cracking loading stages. The iterative register-eliminate algorithm is also
193 shown in Figure 7.

194 Next, actual crack(s) are selected among the possible cracks. The full- and partial-interaction cracking
195 indexes are compared. The first modelled crack forms at which the cracking index is highest. The slip
196 distribution around this crack is determined using PI analysis. All possible cracks falling within the vicinity
197 (slip region) of the newly formed crack are eliminated. The section with the second highest cracking index
198 among the remaining possible cracks is then selected as another actual crack and again all possible cracks
199 in its neighbourhood (slip distribution region) are eliminated.

200 This procedure is continued until all possible cracks are either indicated as actual cracks or eliminated from
201 the calculation. In other words, the calculation stops where there is no possibility for other cracks to form
202 at this stage of loading apart from the actual cracks that are already registered. For additional load
203 increments, the same register-eliminate procedure is applied to find subsequent cracks.

204

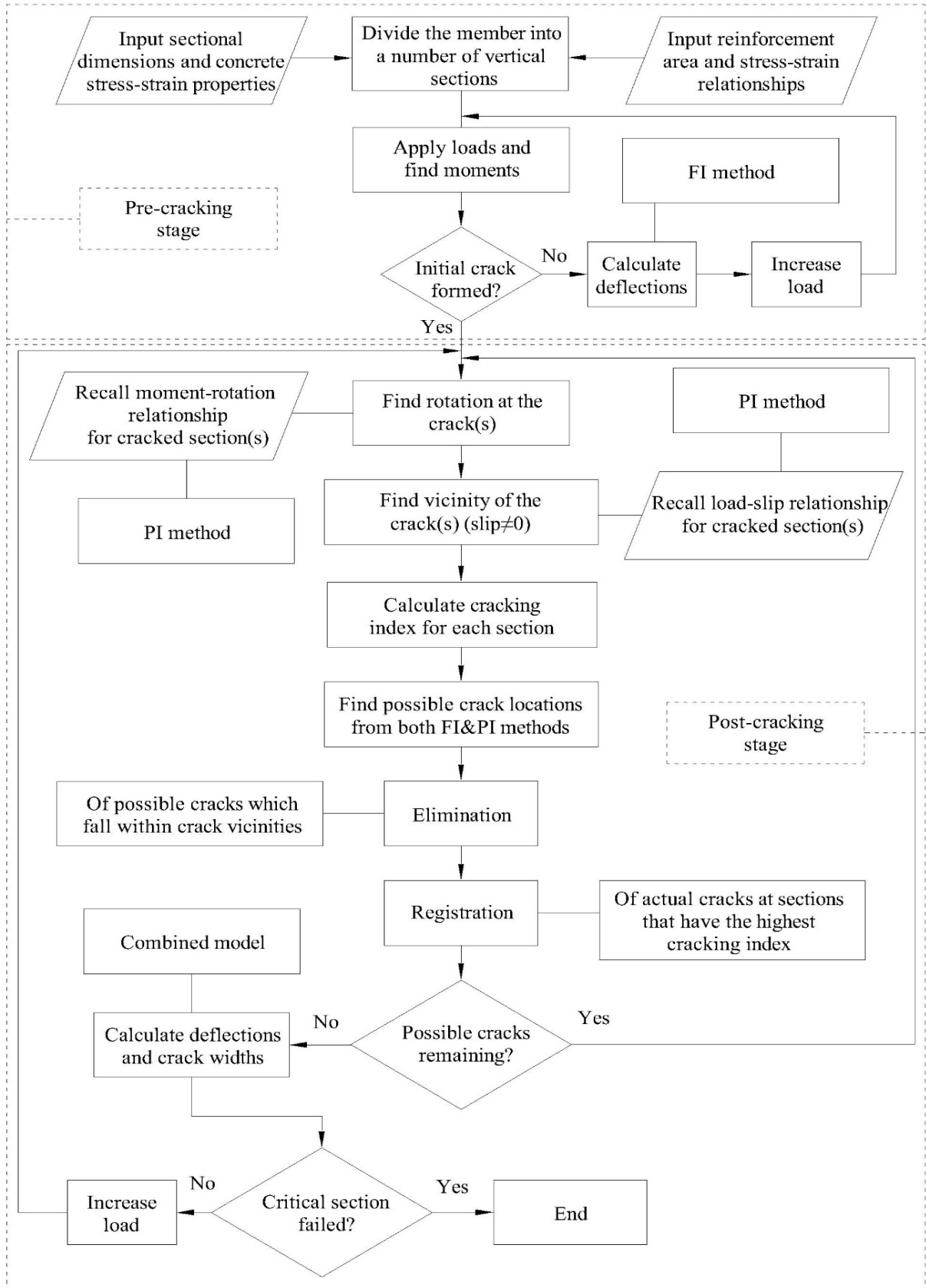


205

206 Figure 6: Register-eliminate method: (a) Non-prismatic beam, (b) Finding possible cracks, (c)

207 Elimination of possible cracks and (d) Registering actual cracks.

208



209

210

Figure 7: Register-eliminate algorithm

211

212 2.3.2 Deflection

213 The deflection profile is found by combining the contribution to deflections from 1) applying the method
214 of double integration of curvatures to the full-interaction regions where curvature has a non-zero value but
215 slip is zero and 2) applying a discrete crack rotation approach at the actual cracks.

216 In the early post-cracking stage, deflection from curvatures dominates since there are fewer cracks and full-
217 interaction regions are wider than partial-interaction regions. At later stages of cracking, however,
218 deflections are mainly governed by rotation of discrete cracks rather than by curvature.

219 Deflection profiles from full-interaction analysis are found by dividing the beam into a number of sections
220 and then recalling moment-curvature relationships for each section, and finding the value of curvature κ
221 corresponding to the applied section moment, M . Once all moment-curvature relationships are known for
222 all sections along the beam, the curvature relating to a specific moment due to loading is integrated once
223 to find the rotations, θ , and these rotations are integrated again to find deflections Δ_f , as described in
224 Equations (3) and (4):

$$225 \quad \theta = \int_{x=0}^{x=L} \kappa dx \quad (3)$$

$$226 \quad \Delta_f = \int_{x=0}^{x=L} \theta dx \quad (4)$$

227 where L is the total length of the beam. A combination of full-interaction and partial-interaction analysis
228 can be used to find deflections as explained below:

$$229 \quad \Delta = \Delta_f + \Delta_p \quad (5)$$

230 where Δ is the total deflection value, Δ_f is the contribution to deflections from flexural curvature for
231 uncracked regions which is determined from equations (3) and (4), and Δ_p is the contribution to deflections
232 from discrete crack rotations for the cracked regions and found as below:

$$233 \quad \Delta_p = \frac{\theta_c L_1 L_2}{L} \quad (6)$$

234 where L_1 and L_2 are distances from the crack to the two supports, and θ_c is the rotation induced by the
235 crack. When calculating Δ_f , it is important to realise that the beam has curvature values in the full-

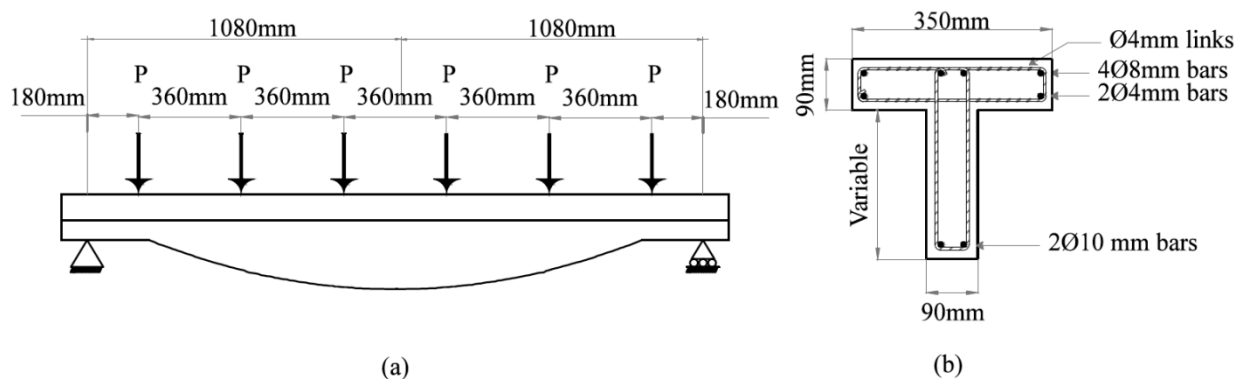
236 interaction regions only, so the value κ should be taken to be zero at those sections that have non-zero
237 values of slip, δ , in the cracked regions as these are accounted for by Δ_p .

238 3 Verification

239 In order to verify the models developed in this paper an experimental program was carried out in which
240 two simply supported T-beams were designed and tested under 8-point loading to approximate uniformly-
241 distributed loading. Figure 8 provides details of the designed beam profiles and cross-sections.

242 The beams were denoted as OS1 and OS2 and had different profiles as they were optimised for different
243 optimisation targets; beam OS1 was optimised for strength only and beam OS2 was optimised for both
244 strength and serviceability. The procedure and results of the optimisation are outside the scope of this paper.
245 Therefore, only the serviceability behaviour of the beams is discussed here.

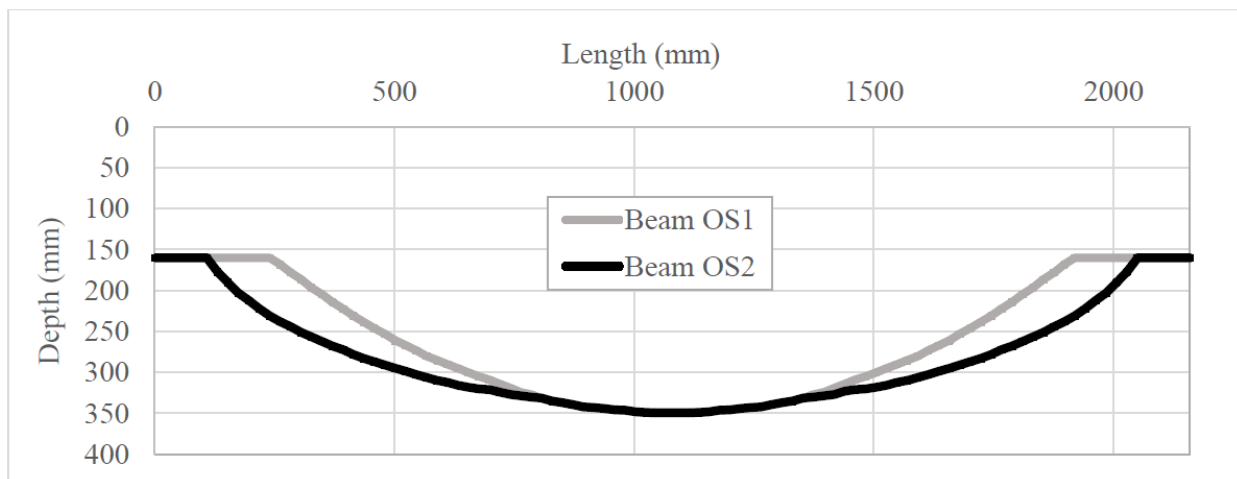
246 The beams were cast in timber moulds using concrete of a cylinder design strength of 30 kN. Beam OS1
247 was tested at the age of 33 days and beam OS2 was tested at 30 days.



248

249

Figure 8: (a) Tested beams profile and test set-up, (b) cross-section of the tested beams



250

251

Figure 9: Profiles of the tested beams optimise for ultimate and serviceability limit states

252

The minimum required depth of the beams near the supports was 160mm to prevent shear failure, and 4mm

253

steel links were placed at 60 mm centres. The as-built longitudinal profiles of the beams are shown in

254

Figure 9. The design limit loads and the predictions of deflections, crack spacing and crack width are shown

255

in Table 1. Since the specimens were subject to laboratory loadings rather than combinations of actual

256

variable and permanent loadings, the service load level is taken to be approximately half of the theoretical

257

ultimate failure load.

258

Table 1: Predicted ultimate and serviceability limit state values

<i>Beam</i>	<i>Failure mode</i>	<i>Failure load (kN)</i>	<i>Service load (kN)</i>	<i>Maximum deflection at 51 kN (mm)</i>	<i>Average crack width at 51 kN (mm)</i>	<i>Total number of cracks under service loads</i>
OS1	Flexure	105	51	2.6	0.13	16
OS2	Flexure	105	51	2.1	0.10	13

259

3.1 Material properties

260

The average yield strength of the longitudinal tension steel bars was 585 MPa and for the compression steel

261

bars it was 510 MPa based on 12 samples for each test. The average cylinder compressive strengths of the

262

concrete for beam OS1 and beam OS2 were 31.7 MPa and 32.6 MPa, respectively, based on three cylinder

263

tests for each beam at the age of 33 and 30 days respectively. The split tensile test was carried out on

264 100X200mm cylinders; the tensile strength values achieved were converted to axial tensile strength
265 according to (BS EN 1992-1-1, 2004) as follows:

266
$$f_{ct} = 0.9f_{ct,sp} \quad (7)$$

267 where f_{ct} is the axial tensile strength and $f_{ct,sp}$ is the split tensile strength of concrete. The concrete tensile
268 strength was 2.65 MPa for beam OS1 and 2.89 MPa for OS2, also based on three test samples for each
269 beam.

270 **3.2 Material constitutive laws and bond-slip model**

271 Standard models provided by BS EN 1992-1-1 (2004) have been used here to represent the stress-strain
272 relationship of concrete (which characterizes strain-softening) and steel bars under uniaxial compressive
273 and tensile stresses, and the commonly used bond-slip model proposed by CEB-FIP (2010) has been
274 adopted.

275 **3.3 Test method**

276 Loads were applied by hydraulic jacks, as shown in Figure 10. At total load increments of 3kN, deflections
277 were measured under each point load. Crack width readings were taken at every load increment using a
278 high definition crack microscope with a precision equal to 0.02mm. The cracks were measured at the level
279 of tensile reinforcement and at exactly the same points in each loading step.



280

281

Figure 10: Test setup for beam OS

282 **3.4 Results**

283 In order to check the validity of the predictions of the combined-interaction method, the data collected from
 284 the tests were compared with the analytical data.

285 The analytical predictions for average and maximum crack widths are compared with the test data for
 286 beams OS1 and OS2 in Table 2 and Table 3 respectively. The cracking data at three stages of loading is
 287 considered to study the cracking process; at the initiation of cracking at 30kN (33kN for beam OS2 as
 288 cracking started at later stages than that of beam OS1), propagation of cracks at 39kN and serviceability,
 289 load limit of 51kN.

290 It can be seen from Table 2 that the prediction of the average crack width values and number of cracks is
 291 reasonably accurate at a load level of 33kN and 39kN. The occurrence of all cracks at this load level was
 292 predicted by the full-interaction mechanism, while the crack width values were calculated from the partial-
 293 interaction analysis, indicating the importance and effectiveness of using a combined approach.

294 Table 2: experimental and predicted crack width and cracks number values for beam OS1

Load	Average crack width (mm)		Maximum crack width (mm)		Number of cracks		Total crack width (mm)		Discrepancy (Total crack width)	Discrepancy (Maximum crack width)
	Exp.	Pred.	Exp.	Pred.	Exp.	Pred.	Exp.	Pred.		
33	0.07	0.08	0.09	0.12	8	12	0.56	0.96	71%	33%
39	0.09	0.10	0.16	0.13	12	14	1.08	1.4	30%	19%
51	0.10	0.13	0.18	0.15	19	16	1.9	2.08	9%	17%

295

296 Table 3: predicted and experimental cracking data of beam OS2

Load	Average crack width (mm)		Maximum crack width (mm)		Number of cracks		Total crack width (mm)		Discrepancy (Total crack width)	Discrepancy (Maximum crack width)
	Exp.	Pred.	Exp.	Pred.	Exp.	Pred.	Exp.	Pred.		
33	0.06	0.07	0.08	0.1	6	9	0.36	0.63	75%	25%
39	0.08	0.1	0.12	0.13	10	11	0.8	1.1	38%	8%
51	0.09	0.1	0.16	0.16	15	17	1.35	1.7	26%	0%

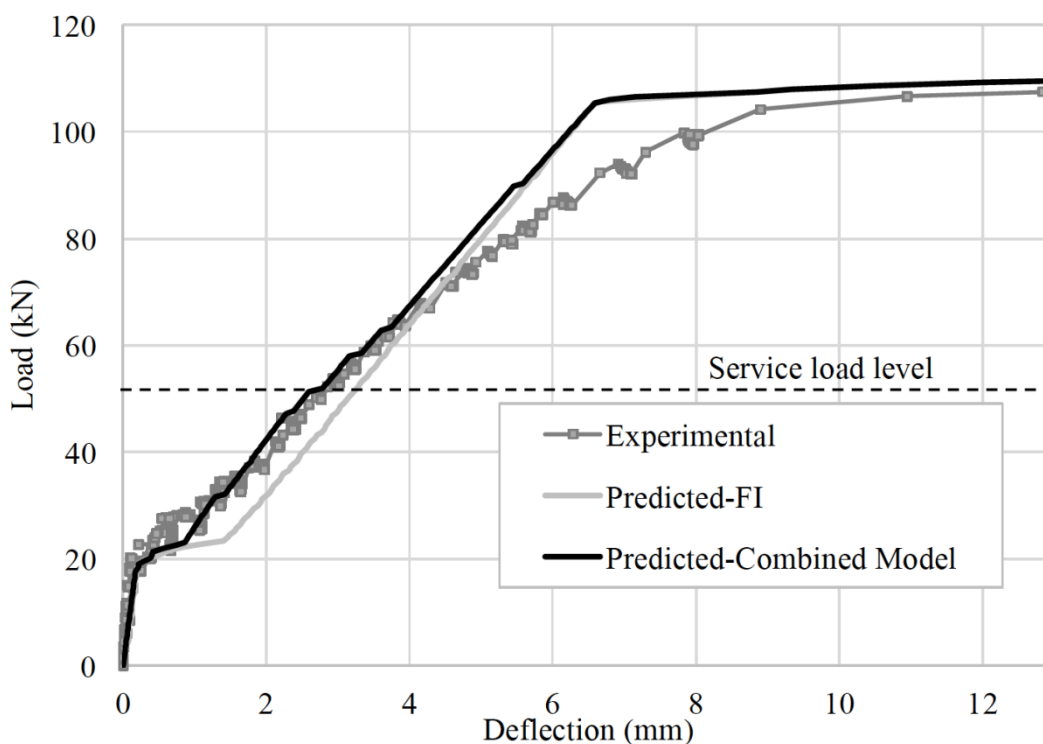
297

298 Despite a slight underestimation in the number of cracks in most cases, the experimental average crack
299 widths and their equivalent predictions are in reasonable agreement.

300 Figures 11 and 12 show the experimental load-deflection relationships compared with the analytical results
301 by the full-interaction and combined-interaction methods for both beams. Here, the load-deflection
302 relationship from the partial-interaction method was not considered for two main reasons: 1) the partial-
303 interaction method is unable to predict load-deflection behaviour of the beams in the pre-cracking stage,
304 and 2) for the non-prismatic beams considered here, a high number of cracks are predicted by the full-
305 interaction mechanism and ignored by the partial-interaction method so that considering the deflection
306 values without accounting for these cracks would not provide a rigorous comparison.

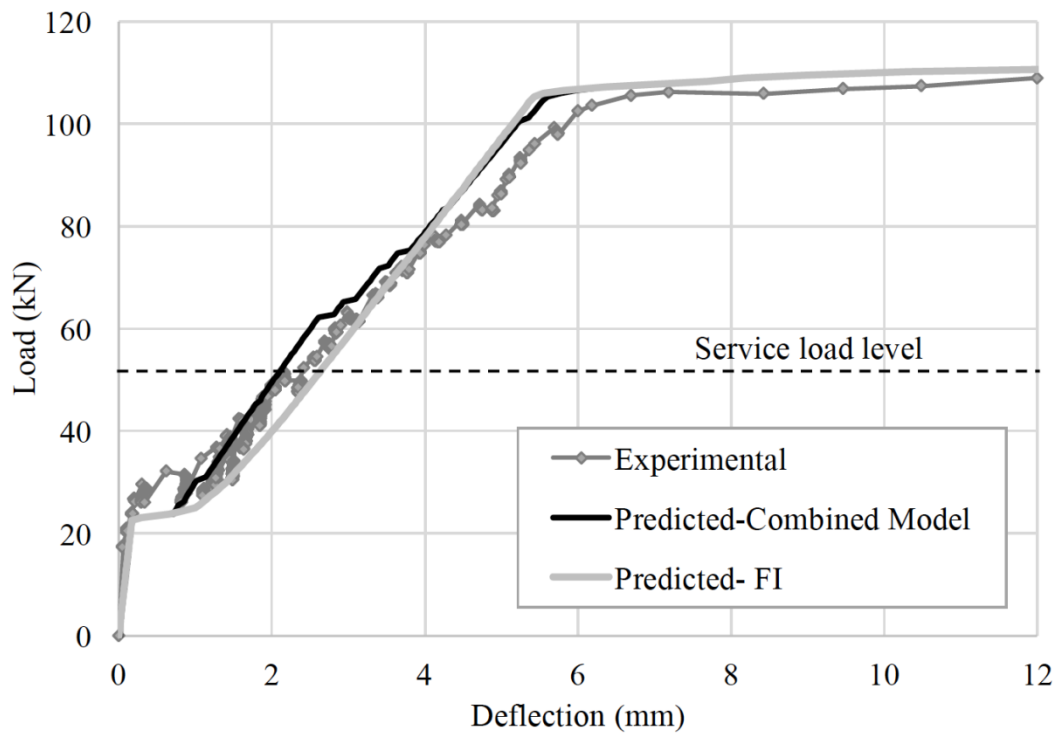
307 There is generally good agreement shown between both methods. The combined-interaction method
308 predicts service-level stiffness and, hence, deflections more accurately than the full-interaction model.

309 There is no discernible difference between the two methods at higher loads.



310

311 Figure 11: Experimental and predicted load deflection curves for beam OS1



312

313 Figure 12: Experimental and predicted load deflection curves for beam OS2

314 4 Conclusions

315 Fabric-formed concrete structures offer the opportunity for a new form of architecture which places
 316 concrete only where it is needed, thereby saving on concrete quantities. But while full strength envelopes
 317 are retained through this approach, overall stiffness of the structure is reduced, so that it is imperative that
 318 an accurate predictor of serviceability criteria is developed in order to verify that fabric-formed concrete
 319 structures will perform adequately. Therefore, numerical models have been developed in this work in order
 320 to predict the behaviour of non-prismatic concrete beams. The prediction model combines full-interaction
 321 analysis (where bond slip is not allowed between the reinforcement and the concrete) and partial-interaction
 322 analysis (where bond-slip may occur).

323 The main conclusions of the work presented in this paper are:

- 324 1- The combined-interaction method developed in this work provides good predictions for deflections
 325 at serviceability as it takes into account bond-slip effects.
- 326 2- In general, predictions for the average and maximum crack widths and the number of cracks are
 327 reasonably accurate when compared with experimental results. At serviceability and for beams

328 OS1 and OS2, the combined-interaction method was approximately 11% and 21% more accurate
329 than the full-interaction method, respectively.

330 This means that for the first time the relevant serviceability criteria for fabric-formed concrete structures
331 of varying geometry may be predicted adequately. This paper deals with simply supported beams only,
332 however, the combined-interaction method can also be used for continuous beams since since different
333 cracking regions along the beam in positive and negative moment areas can be dealt with separately in this
334 new model.

335 Future studies on using the combined interaction method for beams reinforced with FRP bars or other types
336 of reinforcement with different bond-slip properties is suggested as different levels of crack propagation at
337 serviceability can be studied using the proposed method. This paper deals with short-term serviceability
338 behaviour of non-prismatic beams without taking into account creep and shrinkage effects, therefore,
339 further research work considering the effect of these parameters with the proposed combined-interaction
340 model for non-prismatic beams is suggested.

341 **References**

- 342 ACI COMMITTEE 435 (2000). Control of Deflection in Concrete Structures. ACI 435R-95.
- 343 Bailiss, J. (2006). Fabric-Formed Concrete Beams Design and Analysis. Architecture and Civil
344 Engineering, University of Bath. MEng.
- 345 BS EN 1992-1-1 (2004). Eurocode 2: Design of Concrete Structures.
- 346 CEB-FIP (2010). Model Code, Switzerland, International Federation for Structural Concrete (fib).
- 347 Garbett, J. and T. Ibell (2008). Bone Growth Analogy for Optimising Flexibly Formed Concrete Beams.
348 Department of Architecture and Civil Engineering, University of Bath. MEng.
- 349 Hawkins, W., Herrmann, M., Ibell, T., Kromosor, B., Michaelski, A., Orr, J. and Pedreschi, R. (2016)
350 Flexible Form-work Technologies - A State of the Art Review. Structural Concrete, 17(6).
- 351 Kwak, H.-G. and S.-P. Kim (2002). Non-Linear Analysis of RC Beams Based of Moment-Curvature
352 Relation. Computers & Structures 80, 615-628.

353 Oehlers, D. J., Muhamad, R. and Mohamed Ali, M. S. 2013. Serviceability Flexural Ductility of FRP RC
354 Beams: A Discrete Rotation Approach. *Construction and Building Materials*, 49, 974-984.

355 Oehlers D. J., et al. (2011). FRP-Reinforced Concrete Beams: Unified Approach Based on IC Theory.
356 *Journal of Composites for Construction* 15(3), 293-303.

357 Orr, J. (2012). Flexible Formwork for Concrete Structures. *Architecture and Civil Engineering*,
358 University of Bath. PhD.

359 Tayfur, Y. (2017). Optimisation for Serviceability of Fabric-formed Concrete Structures. *Architecture*
360 *and Civil Engineering*, University of Bath. PhD thesis.

361 Veenendal, D., West, M. and Block, P. (2011). History and Overview of Fabric Formwork: Using Fabrics
362 for Concrete Casting. *Structural Concrete* 12(3), 164-177.

363 Visintin, P., Oehlers, D. J., Muhamad, R. and Wu, C. (2013). Partial-interaction Short Term
364 Serviceability Deflection of RC Beams. *Engineering Structures*, 56, 993-1006.

365

366